



# 2D-DIGE proteomic analysis reveals changes in haemolymph proteome of 1-day-old honey bee (*Apis mellifera*) workers in response to infection with *Varroa destructor* mites

Mariola SŁOWIŃSKA<sup>1</sup>, Joanna NYNCA<sup>1</sup>, Beata BAŁ<sup>2</sup>, Jerzy WILDE<sup>2</sup>, Maciej SIUDA<sup>2</sup>, Andrzej CIERESZKO<sup>1</sup>

<sup>1</sup>Department of Gamete and Embryo Biology, Institute of Animal Reproduction and Food Research, Polish Academy of Sciences in Olsztyn, Tuwima 10, 10-748, Olsztyn, Poland

<sup>2</sup>Department of Apiculture, Faculty of Animal Bioengineering, University of Warmia and Mazury in Olsztyn, Słoneczna 48, 10-957, Olsztyn, Poland

Received 1 February 2019 – Revised 29 May 2019 – Accepted 2 July 2019

**Abstract** – *Varroa destructor* is an external parasite of *Apis mellifera* and feeds on the haemolymph of pupae and adult bees, vectoring numerous viral pathogens, in particular the deformed wing virus (DWV). However, the changes in haemolymph protein composition after *Varroa* infestation are unknown. The objective of this study was to investigate alterations in the haemolymph proteome in relation to *Varroa* parasitism. Using two-dimensional difference gel electrophoresis and MALDI-TOF/TOF mass spectrometry, we identified changes in 44 haemolymph proteins in response to the parasite and one in protein originated from DWV. The following pathways were affected by *Varroa* infestation, including carbohydrate metabolism, detoxification and oxidative stress response, nutrient reservoir activity, oxidoreductase activity and the olfactory system. Several physiological functions of honey bees, such as energy metabolism, detoxification, metamorphosis and chemosensing, may be disrupted by *Varroa*.

*Apis mellifera* / *Varroa destructor* / haemolymph / proteome / DIGE

## 1. INTRODUCTION

The *Varroa* mite (*Varroa destructor*) is an external parasite of the honey bee (*Apis mellifera*) and feeds on the haemolymph of pupae and adult bees (Nazzi and Le Conte 2016). However, it has been recently suggested that *Varroa* feeds primarily on honey bee fat body tissue (Ramsey et al.

2019). *Varroa* has successfully shifted from the original host, *Apis cerana*, to the Western honey bee, *Apis mellifera*, in the 1950s (Villalobos 2016). *Apis mellifera* is not well adapted to the mite, and infested colonies suffer severe damage (Oldroyd 1999). The damage caused by *Varroa* to the colonies is not strictly related to the parasitic action of the mite, as it also vectors numerous honey bee viral pathogens, such as deformed wing virus (DWV) (De Miranda and Genersch 2010; Wilfert et al. 2016), the member of the iflavirus group, also including slow bee paralysis virus (Kalynych et al. 2016), sacbrood virus (Ryabov et al. 2016) and Moku virus (Mordecai et al. 2016). The *Varroa* mite, in combination with its associated viruses, most notably DWV, has been

**Electronic supplementary material** The online version of this article (<https://doi.org/10.1007/s13592-019-00674-z>) contains supplementary material, which is available to authorized users.

Corresponding author: M. Słowińska,  
m.slowinska@pan.olsztyn.pl  
Manuscript editor: Yves Le Conte

associated with the death of millions of European honey bee colonies across the world (Brettell and Martin 2017).

The physical and physiological effects of *Varroa* on individual bees have been extensively investigated, and considerable pathological effects of mites on honey bees have been reported. Lower protein concentrations and carbohydrate concentrations were found in the bodies of emerged parasitised bees (Bowen-Walker and Gunn 2001). *Varroa* parasitism causes direct harm to developing bees in terms of reduced emergence body weight and metabolic reserves, pupal and adult weight loss, brood developing into adults with shorter abdomens, deformed wing and shorter life spans and behavioural changes including altered flight duration and homing ability of infested foragers (De Jong et al. 1982; Allen and Ball 1996; Duay et al. 2003; Bowen-Walker and Gunn 2001; Kralj and Fuchs 2006). Knowledge regarding the mechanism of those pathological effects is crucial to improve our understanding of *Varroa* parasitism and important for the diagnosis, prevention and treatment of *Varroa*.

Recently, proteomics analysis has been used in studies of *Varroa destructor* mites (Erban et al. 2015; McAfee et al. 2017; Iovinella et al. 2018). Several groups of proteins were identified in *Varroa* females, as follows: (i) proteins of virions such as *Varroa destructor* Macula-like virus, DWV and acute bee paralysis virus (Erban et al. 2015); (ii) a variety of honey bee haemolymph proteins, including apolipoprotein, hexamerins and various major royal jelly proteins (Erban et al. 2015); and (iii) key proteins that may act as semiochemical carriers, such as odorant-binding proteins and Niemann-Pick family, type C2 proteins (Iovinella et al. 2018). However, to our knowledge, no proteomics studies have been conducted in haemolymph of infested honey bees focusing on proteins of *Varroa* origin. The presence of *Varroa*-borne proteins and transmitted viruses may be expected in honey bee haemolymph (Bogaerts et al. 2009; Dainat et al. 2012; Erban et al. 2015).

Honey bee haemolymph plays a role in immune defence and is also vital for daily life functions, such as transport of nutrients and signalling molecules (Erban et al. 2016). Several proteomic

approaches have been used to investigate caste differences (Chan et al. 2006; Ararso et al. 2018) and developmental changes in honey bee haemolymph (Bogaerts et al. 2009; Erban et al. 2014, 2016; Feng et al. 2014). Proteome analysis of larvae as well as of the haemolymph, mushroom body, head tissues and antenna provides novel insights into honey bee resistance against *Varroa* infestation (Parker et al. 2012; Ji et al. 2015; Hu et al. 2016). Moreover, quantitative proteomics was applied to reveal divergent responses in worker and drone pupae to parasitisation by *Varroa*. Proteins involved in fatty acid metabolism and carbohydrate metabolism were more abundant in parasitised workers in comparison to drones (Surlis et al. 2017). However, present knowledge regarding honey bee responses to *Varroa* is restricted to whole pupae.

The objective of this study was to compare the proteomes of haemolymph of non-infested honey bees with those of bees parasitised with one or more (2–3) *Varroa* mother mites, using two-dimensional difference gel electrophoresis (2D-DIGE) to quantify proteins and matrix-assisted laser desorption/ionisation (MALDI) mass spectrometry to identify proteins with different abundances in haemolymph.

## 2. MATERIALS AND METHODS

### 2.1. Sample collection

Four honey bee (*Apis mellifera carnica* L.) colonies were assigned to the experiment, in which *Varroa destructor* was not controlled for 2 years. At this time, acaricides were not used in bee colonies from which the research material was obtained. Therefore, the colonies were characterised by high infection rates with this parasite (on average, 12%). From these colonies, during the period from 06 April 2017 to 23 April 2017, combs with sealed brood, 2–3 days before emerging, were taken out and transferred into an incubator (35 °C, humidity 60%). Every hour, the sealed brood were observed and workers which had already emerged were picked out to check if they were infected with parasites. The cells were also monitored for the presence of *Varroa*. Individual workers were partitioned into different

groups: control group—workers free from parasites or infested with one (V1) or two to three (V2–3) mother females of *Varroa*. Collected workers were kept in a Fotie cage in an incubator until used for haemolymph collection. This took place within 24 h from the moment the workers emerged from the comb cells. Bees from all three groups [non-infested honey bees, bees parasitised with one and more (2–3) *Varroa* mother mites] underwent the same treatments in laboratory conditions in order to exclude changes in physiology/bee proteome caused by differences in bee brood breeding.

Haemolymph was collected from the head, using the novel antennae method for haemolymph sampling (Borsuk et al. 2017). Approximately 10  $\mu$ L of transparent haemolymph was collected from each individual. The samples from three to four honey bees were pooled in a 1.5-mL Eppendorf tube on ice until 40  $\mu$ L was collected. Eighteen pooled samples were prepared, consisting of six samples for the control, six samples of bees infested with one *Varroa* mother mite and six samples of bees infested with two to three *Varroa* mother mites. To prevent proteolysis and melanisation, which is connected to a serine protease and prophenoloxidase, a protease inhibitor cocktail (1:100, P8340, Sigma-Aldrich, Saint Louis, MO, USA) with the following composition 104 mM AEBSF, 80  $\mu$ M aprotinin, 4 mM bestatin, 1.4 mM E-64, 2 mM leupeptin and 1.5 mM pepstatin A was added to the haemolymph. The addition of cocktail to haemolymph decreased the melanisation process of haemolymph (Słowińska et al., unpublished observation). The samples were immediately frozen at  $-80^{\circ}\text{C}$ .

## 2.2. Sample preparation

Haemolymph proteins were precipitated using the 2-D Clean-up Kit (GE Healthcare, Uppsala, Sweden). The pellet was re-suspended in DIGE labelling buffer consisting of 30 mM Tris, 7 M urea, 2 M thiourea and 4% CHAPS. The protein concentration was measured by the method of Bradford (1976), using a Coomassie Plus Kit (Thermo Scientific, Waltham, MA, USA) with bovine serum albumin as standard.

## 2.3. Fluorescence labelling of haemolymph proteins with CyDyes and 2D-DIGE

Six biological replicates for each treatment (6 biological replicates  $\times$  3 treatments = 18 samples) were used for 2D-DIGE experiment. Protein labelling with CyDye DIGE fluor and 2D electrophoresis was performed under the same conditions as described by Słowińska et al. (2015). Briefly, 50  $\mu$ g of each sample was minimally labelled by incubation with 400 pmol of amine-reactive cyanine dye (Cy3 or Cy5) on ice for 30 min in the dark. At the same time, the internal standard sample was generated by combining equal amounts of proteins from each of the 18 samples (labelled with Cy2) for a ratio of 50  $\mu$ g protein to 400 pmol Cy2. The arrangement of the haemolymph samples for the 2D-DIGE experiment is shown in Supplementary Table S1. The samples were then loaded onto IPG strips (24 cm, pH 3–10, NL; GE Healthcare) with passive rehydration (18 h). Isoelectric focusing was performed with an IPGphor isoelectric focusing unit (GE Healthcare) and SDS-PAGE was run using the ETTAN Dalt six electrophoresis unit (GE Healthcare) as described by Słowińska et al. (2015).

The DIGE technique used in our study requires only biological replicates, since gel-to-gel variation is virtually eliminated with this technique by the presence of a pooled internal standard. The pooled internal standard was a combination of equal aliquots of each sample that was analysed in the experiment, as recommended by Beckett (2012). The pooled standard is used to help normalise the signal between and within each gel by comparing the ratio of each labelled protein spot to the internal standard and then to the same protein spot in the other gels. In addition, the pooled internal standard is used as a standard map to match protein spots across multiple gels, since all of the spots in the internal standard should be present across all of the gels.

## 2.4. Image acquisition and quantitative analysis

The CyDye-labelled gels analysed by fluorescence imaging with the use of Typhoon FLA 9500

(GE Healthcare) are presented in Supplementary Fig. S1. Image analysis was performed with the use of DeCyder Differential Analysis Software (Version 5.02 software, GE Healthcare). All spots with a  $p$  value lower than 0.05 were considered as differentially abundant and were used for further analysis (Cardoen et al. 2012). After DIGE analysis, gels were stained with Coomassie Brilliant Blue R-250 or silver stained (Bio-Rad, Hercules, CA, USA) according to the following studies: Tonge et al. (2001), Vierstraete et al. (2004) and Dautel et al. (2011). The 2D-DIGE gels stained with Coomassie Brilliant Blue R-250 or silver stained are presented in Supplementary Fig. S2. Such gels were used for manual protein spot picking.

## 2.5. MALDI-TOF/TOF protein identification

Spots of interests were cut manually from the gel and subjected to reduction, alkylation and in-gel trypsin digestion as described by Słowińska et al. (2014). The peptides were concentrated and desalted using ZipTip pipette tips (Sigma-Aldrich), which had been first equilibrated by sequential washings with 100% acetonitrile (ACN), then with 50% ACN, 0.1% trifluoroacetic acid (TFA) and finally with 0.1% TFA. The digested peptides were loaded onto the ZipTip and contaminants were washed away with 0.1% TFA. Peptides were eluted with 1  $\mu$ L of matrix solution containing 5 mg of  $\alpha$ -cyano-4-hydroxycinnamic acid (Bruker Daltonics, Bremen, Germany) in 1 mL of 50% ACN and 0.1% TFA. This was spotted directly onto a steel MALDI target plate (MT 34 Target Plate Ground Steel, Bruker Daltonics). Additionally, a peptide calibration standard (Bruker Daltonics) was spotted using the dried-droplet method with the matrix for calibration of the mass spectrometer. The peptide calibration standard was composed of a mixture of the following peptides with monoisotopic  $[M+H]^+$   $m/z$  values: bradykinin 1–7 [757.3992], angiotensin II [1046.5418], angiotensin I [1296.6848], substance P [1347.7354], bombesin [1619.8223], ACTH clip 1–17 [2093.0862], ACTH clip 18–39 [2465.1983] and somatostatin 28 [3147.4710].

Mass spectra were acquired in the range of 500–3500  $m/z$ , using an MALDI-TOF AutoFlex Speed TOF/TOF mass spectrometer equipped with a Smartbeam II laser (355 nm, Bruker Daltonics). Operating conditions were as follows: laser frequency = 1000.0 Hz, ion source 1 = 19.10 kV, ion source 2 = 16.80 kV, lens voltage = 7.50 kV, reflector voltage = 20.99 kV, reflector 2 voltage = 9.59 kV, optimised pulsed ion extraction time = 120 ns, matrix suppression = 500 Da and positive reflectron mode was used. The strongest precursors were selected for MS/MS analysis with the following operating conditions: detection range = 40–2285 Da, laser frequency = 200.0 Hz, ion source 1 = 6.04 kV, ion source 2 = 5.34 kV, lens voltage = 3.00 kV, reflector voltage = 26.99 kV, reflector 2 voltage = 11.59 kV, lift 1 voltage = 18.96 kV, lift 2 voltage = 4.00 kV, optimised pulsed ion extraction time = 130 ns and positive reflectron mode was used.

Peptide masses from mass spectrometry analysis and their fragments obtained from MS/MS spectra were combined and submitted to bioanalyses searched using Mascot Server (Matrix Science, London, UK) and NCBI as the database. The database search criteria were as follows: enzyme: trypsin, fixed modification: carbamidomethylation (C) and variable modifications: oxidation (M) peptide mass tolerance of 200 ppm, fragment mass tolerance of 0.7 Da and one missed cleavage allowed, which is within the range recommended by Gasteiger et al. (2005). The search results were filtered with a significant threshold of  $p < 0.05$  and a MASCOT ion score cut-off of  $\geq 30$ . The following criteria for protein identification, which followed the recommendations of Barceló-Batllori et al. (2008), were applied in our study: (i) matches considered statistically significant ( $p < 0.05$ ) by Mascot with at least two correctly identified parent ions were regarded as correct hits; (ii) when non-homologous proteins were identified in one spot for the correct identification, we chose a protein which had a score of at least two orders higher than the next hit and the most abundant peptides in the spectra were assigned as the identified protein; (iii) when the highest score matched the same protein from several honey bee species, the taxonomy *Apis mellifera* was selected because this was the origin

of the sample; otherwise, the identity of the first species was reported; and (iv) searches that did not meet the criteria described above were further reanalysed by MS/MS using MALDI-TOF/TOF. Raw MALDI-TOF/TOF data have been deposited to the ProteomeXchange Consortium via the PRIDE (Vizcaíno et al. 2016) partner repository with the dataset identifier PXD012429.

## 2.6. Classification of differentiated haemolymph proteins

Classification of differentiated proteins was performed involving the following steps: (i) to obtain Gene Ontology annotation for biological processes and molecular functions, the GI numbers of identified proteins were mapped to the UniProtKB database ([www.uniprot.org](http://www.uniprot.org)) and honey bee was selected as organism; (ii) for proteins with unknown function in honey bees, *Drosophila melanogaster* was used as the insect organism model; and (iii) in the case of proteins whose functions were unknown in insects, the function was speculated based on published data.

Using the Ingenuity Pathway Analysis package (IPA; Ingenuity, Mountain View, CA), gene names of identified honey bee proteins were used to generate networks. IPA only accepts identifiers for human, mouse or rat. Therefore, orthologues of the identified honey bee proteins belonging to humans were first identified and the gene name of the top blast hits were uploaded to IPA (21 identifiers were mapped by IPA from 44 identified proteins).

## 3. RESULTS

### 3.1. 2D-DIGE comparison of haemolymph of honey bee infested with *Varroa* mother mites

Fifty-six protein spots differed significantly ( $p$  value  $< 0.05$ ) between haemolymph of non-infested bees and of bees infested with one *Varroa* mite (Figure 1). Thirty-four spots representing 23 proteins were enriched in infested honey bees and 22 spots representing 12 proteins were more abundant in non-infested honey bee haemolymph (Table I).

Our analysis showed that 40 protein spots were of different abundance between haemolymph of non-infested bees and infested with two to three *Varroa* mother mites (Figure 2). Twenty-seven spots representing 29 proteins were enriched in infested honey bees and 13 spots representing 5 proteins were more abundant in non-infested honey bee haemolymph (Table I).

Three protein spots representing three proteins were found of different abundance in honey bees infested with two to three *Varroa* mites in comparison to one *Varroa* mite (Figure 3). Two of them were more abundant and one protein was less abundant in the haemolymph of more infected honey bees (Table I). Detailed information on the identification of honey bee haemolymph proteins is presented in Supplementary Table S2.

Hexamerin 110 [BAI82214.1; ratio from +4.84 to +4.71 (V2–3 vs control) and ratio +2.57 (V1 vs control)], cuticular protein precursor [NP\_001167611.1; ratio +3.60 (V2–3 vs control)] and hexamerin [ABR45905.1, ABR45904.1; ratio from +3.25 to +2.62 (V2–3 vs control)] showed the largest increase after *Varroa* infection. Apart from the above-mentioned honey bee proteins that increased in response to *Varroa* infection, a DWV protein, polyprotein (ASU06760.1), was also detected in honey bee haemolymph (average ratio from +2.21 to +1.48, after infestation with one or more *Varroa*, respectively). We did not find the presence of proteins originating from viruses other than DWV in honey bee haemolymph. Neutral alpha-glucosidase AB isoform X1 [XP\_016772970.1; ratio –2.05 (V1 vs control)], neutral alpha-glucosidase AB isoform X2 [XP\_016772970.1; ratio –2.04 (V1 vs control)], odorant-binding protein 14 precursor [NP\_001035313.1; ratio from –1.56 to –1.53 (V2–3 vs control)] and protein disulfide-isomerase A3 [XP\_623282.1; ratio –1.51 (V2–3 vs V1)] showed the most significant decrease after *Varroa* infection. A list of differentially abundant proteins in haemolymph of honey bees after infestation with *Varroa* mother mites in terms of protein ratio values [from the most increased ratio (+4.84) and the most decreased ratio (–2.05)] for the three sets of data (V1 vs control; V2–3 vs control; and V2–3 vs V1) is presented in Table II.

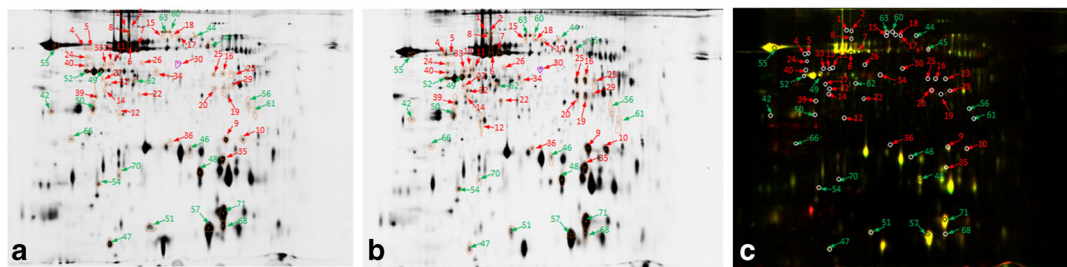


**Figure 1.** Two-dimensional difference gel electrophoresis (2D-DIGE) analysis of honey bee haemolymph proteins after infestation with one *Varroa* mother mite. **a** Single-channel image of proteins from control haemolymph. **b** Single-channel image of proteins from haemolymph after one *Varroa* mother mite infestation. **c** Overlay of Cy3 and Cy5 channel images according to haemolymph arrangement presented in Supplementary Table S1 for gel no. 2. Numbered protein spots (red) correspond to the proteins identified from 2D-DIGE that are more abundant after *Varroa* infestation and (green) indicate the identified spots that are more abundant in uninfected honey bees. Results of spot identification are presented in Table I. **a, b** Originated directly from Biological Variation Analysis workspace of DeCyder Differential Analysis Software. **c** Originated from Image Quant TL; the differentiated proteins were marked manually in order to improve spot marking.

### 3.2. Analysis of proteins showing changes in abundance

Results of classification of molecular function of differentiated proteins are presented in Table III. Haemolymph proteins that showed changes in abundance between uninfected and parasitised honey bees were involved in the following physiological processes: carbohydrate metabolism, detoxification and oxidative stress response, chemosensing and nutrient reservoir. Moreover, several proteins were classified as proteins with oxidoreductase activities. The graphical presentation of molecular function is presented in Figure 4. The top canonical pathways mapped by IPA were mainly connected with carbohydrate metabolism. The results of IPA analysis with statistical representation are presented in Table IV.

## 4. DISCUSSION

### 4.1. Polyprotein of deformed wing virus in honey bee haemolymph—a sign of *Varroa* infestation

In this study, we identified, using proteomics, DWV (polyprotein ASU06760.1) in the haemolymph of honey bees infested with *Varroa* mites. It is well documented that *Varroa*, which

feeds on honey bee haemolymph, is a major vector for viral pathogen transmission, in particular the iflavivirus DWV (Wilfert et al. 2016). According to Erban et al. (2015), the mite transmits the virus—directly to the haemolymph, which is enough to facilitate the viral infection (Erban et al. 2015). In the absence of *Varroa*, DWV normally persists at low levels within honey bee colonies, with no detrimental effect, and can be found in all life stages (Chen et al. 2005, 2006; Yue and Genersch 2005; Bogaerts et al. 2009). The increased level of DWV polyprotein in the haemolymph of infested honey bees in our study provides strong evidence for an active role of *Varroa* in the transmission of DWV of honey bee colonies within our experiment. As such, the observed changes in protein abundance in the haemolymph of honey bees infested with *Varroa* can be attributed both to the potential action of *Varroa* as well as to the action of DWV.

An increased level of polyprotein derived from DWV was found in honey bee haemolymph after infestation with one (ratio +2.21) or two/three (+1.48) *Varroa* mother mites in comparison to non-infested honey bees. Interestingly, no statistically significant differences in polyprotein were found between bees infested with one mite and two/three mites. The lack of an increased level of polyprotein after infestation with several mites can be explained by the results of Bowen-Walker et al.

**Table I.** List of differentially expressed proteins in haemolymph of honey bees infested with *Varroa* mother mites

Pos.	Protein name (organism)	Accession no.	Protein score	No peptides (ion score > 30)	<i>t</i> test	Ratio <sup>1</sup>		
						V1 vs control	V2–3 vs control	V2–3 vs V1
1	Hexamerin 110 ( <i>Apis mellifera</i> )	BAI82214.1	1010	9	0.014	2.15	4.84	
2	Hexamerin 110 ( <i>Apis mellifera</i> )	BAI82214.1	491	5	0.0032	2.57	4.71	
3	Cuticular protein precursor ( <i>Apis mellifera</i> )	NP_001167611.1	142	2	0.00066		3.60	
4	Hexamerin ( <i>Apis mellifera</i> )	ABR45905.1	538	7	0.0028	2.08	3.25	
5	Unidentified				0.0043	1.76	3.01	
6	Hexamerin ( <i>Apis mellifera</i> )	ABR45904.1	615	5	0.019	1.87	2.62	
7	Hexamerin 70a precursor ( <i>Apis mellifera</i> )	NP_001104234.1	427	3	0.023	1.89	2.26	
8	Hexamerin 70a precursor ( <i>Apis mellifera</i> )	NP_001104234.1	577	4	0.013	2.01	2.22	
9	PREDICTED: dehydrogenase/reductase SDR family member 11-like ( <i>Apis dorsata</i> )	NP_001011620.1	290	2	0.0010	2.27	1.90	
10	Short-chain dehydrogenase/reductase ( <i>Apis mellifera</i> )	NP_001011620.1	376	4	0.00065	2.35	1.83	
11	PREDICTED: PTS-dependent dihydroxyacetone kinase, dihydroxyacetone-binding subunit DhaK-like ( <i>Apis mellifera</i> )	XP_397138.5	346	2	0.016	2.19	1.81	
12	PREDICTED: sorbitol dehydrogenase-like ( <i>Apis mellifera</i> )	XP_392401.3	316	4	0.021	1.97	1.78	
13	PREDICTED: PTS-dependent dihydroxyacetone kinase, dihydroxyacetone-binding subunit DhaK-like ( <i>Apis mellifera</i> )	XP_397138.5	134	2	0.0051	2.06	1.77	
14	PREDICTED: uncharacterized oxidoreductase YrbE-like ( <i>Apis mellifera</i> )	XP_624408.2	207	2	0.0070	1.90	1.74	
15	PREDICTED: glycogen phosphorylase ( <i>Apis mellifera</i> )	XP_006561774.1	241	3	0.025	1.76	1.66	
16	PREDICTED: retinal dehydrogenase 1 ( <i>Apis mellifera</i> )	XP_392104.4	506	5	0.028	2.17	1.65	
17	PREDICTED: cytosolic 10-formyltetrahydrofolate dehydrogenase ( <i>Apis mellifera</i> )	XP_006563850.1	233	2	0.013	1.90	1.62	
18	PREDICTED: cytosolic 10-formyltetrahydrofolate dehydrogenase ( <i>Apis mellifera</i> )	XP_006563850.1	239	2	0.025	1.58	1.55	
19	PREDICTED: beta-ureidopropionase ( <i>Apis mellifera</i> )	XP_392773.3	344	4	0.070	2.10		
20	PREDICTED: beta-ureidopropionase ( <i>Apis mellifera</i> )	XP_392773.3	311	4	0.015	1.68	1.53	
21	PREDICTED: 3-ketoacyl-CoA thiolase, mitochondrial ( <i>Apis mellifera</i> )	XP_391843.1	228	3	0.023		1.51	
22	Unidentified					1.90		
23	Polyprotein, partial ( <i>Deformed Wing Virus</i> )	ASU06760.1	230	3	0.046	2.21	1.48	

**Table I** (continued)

Pos.	Protein name (organism)	Accession no.	Protein score	No peptides (ion score > 30)	<i>t</i> test	Ratio <sup>1</sup>		
						V1 vs control	V2–3 vs control	V2–3 vs V1
24	PREDICTED: transketolase-like protein 2 isoform X2 ( <i>Apis mellifera</i> )	XP_623196.3	398	2	0.028	1.74	1.45	
25	PREDICTED: retinal dehydrogenase 1 ( <i>Apis mellifera</i> )	XP_392104.4	695	8	0.20	2.04		
26	PREDICTED: T-complex protein 1 subunit zeta ( <i>Apis florea</i> )	XP_012349557.1	120	2	0.0015	1.53	1.38	
27	PREDICTED: 6-phosphogluconate dehydrogenase, decarboxylating ( <i>Apis mellifera</i> )	XP_006566986.1	195	2	0.072	1.65		
28	Unidentified							1.31
29	PREDICTED: beta-ureidopropionase ( <i>Apis mellifera</i> )	XP_392773.3	208	3	0.084	1.61		
30	PREDICTED: phosphoglucomutase isoform X1 ( <i>Apis mellifera</i> )	XP_395366.2	131	2	0.22	1.57		
31	PREDICTED: fructose-bisphosphate aldolase ( <i>Apis mellifera</i> )	XP_623342.2	261	4	0.036		1.26	
32	PREDICTED: isocitrate dehydrogenase (NADP) cytoplasmic ( <i>Apis mellifera</i> )	XP_623673.3	277	2	0.16	1.48		
33	Carboxylesterase ( <i>Apis mellifera</i> )	NP_001136081.1	365	3	0.11	1.37		
34	Hexamerin ( <i>Apis mellifera</i> )	ABR45904.1	570	4	0.25	1.36		
35	PREDICTED: glutathione S-transferase S1 isoform X1 ( <i>Apis mellifera</i> )	XP_016772844.1	710	7	0.097	1.50		
36	Peroxiredoxin-like protein ( <i>Apis mellifera</i> )	NP_001164444.1	274	4	0.23	1.45		
37	PREDICTED: beta-glucuronidase ( <i>Apis mellifera</i> )	XP_016769246.1	541	4	0.11			1.24
38	PREDICTED: aldose 1-epimerase isoform X1 ( <i>Apis mellifera</i> )	XP_016772523.1	130	2	0.040		1.14	
39	PREDICTED: fructose-bisphosphate aldolase ( <i>Apis mellifera</i> )	XP_623342.2	351	5	0.30	1.85		
40	PREDICTED: glucose-6-phosphate isomerase ( <i>Apis mellifera</i> )	XP_623552.1	409	3	0.16	1.31		
41	PREDICTED: aldose 1-epimerase isoform X2 ( <i>Apis mellifera</i> )	XP_016772524.1	622	6	0.029		1.13	
42	PREDICTED: chitobiosyldiphosphodichol beta-mannosyltransferase-like ( <i>Apis mellifera</i> )	XP_016770702.1	159	2	0.87	-1.41		
43	PREDICTED: serine protease ester ( <i>Apis mellifera</i> )	XP_006570266.1	501	6	0.86			1.19
44	PREDICTED: membrane metallo-endopeptidase-like 1 isoform X2 ( <i>Apis mellifera</i> )	XP_006566920.1	167	2	0.55	-1.22		
45	Unidentified				0.54	-1.30		
46	PREDICTED: circadian clock-controlled protein ( <i>Apis mellifera</i> )	XP_001122696.1	187	2	0.47	-1.21		
47	Unidentified				0.61	-1.42		
48	Unidentified				0.17	-1.19		
49	PREDICTED: chitinase-like protein Idgf4 isoform X1 ( <i>Apis mellifera</i> )	XP_016773072.1	666	6	0.49	-1.37		
50		XP_016772428.1	412	3	0.14	-1.19		



**Table I** (continued)

Pos.	Protein name (organism)	Accession no.	Protein score	No peptides (ion score > 30)	<i>t</i> test	Ratio <sup>1</sup>		
						V1 vs control	V2-3 vs control	V2-3 vs V1
51	PREDICTED: insulin-like growth factor-binding protein complex acid labile subunit ( <i>Apis mellifera</i> )	XP_392381.3	103	2	0.23	-1.22		
52	PREDICTED: putative cysteine proteinase CG12163 isoform X2 ( <i>Apis mellifera</i> )	XP_016769016.1	509	5	0.36	-1.40		
53	Unidentified				0.014		-1.14	
54	PREDICTED: putative defense protein 3 ( <i>Apis mellifera</i> )	XP_003249096.1	198	2	0.15	-1.28		
55	PREDICTED: LOW QUALITY PROTEIN: apolipoporphins ( <i>Apis mellifera</i> )	XP_016768851.1	1030	9	0.19	-1.32		
56	Unidentified				0.083	-1.33		
57	PREDICTED: general odorant-binding protein 56d-like ( <i>Apis cerana</i> )	XP_016915059.1	616	7	0.049	-1.24		
58	Unidentified				0.041		-1.22	
59	PREDICTED: protein disulfide-isomerase A3 ( <i>Apis mellifera</i> )	XP_623282.1	295	3	0.37			-1.51
60	PREDICTED: neutral alpha-glucosidase AB isoform X1 ( <i>Apis mellifera</i> )	XP_016772970.1	462	4	0.36	-2.05		
61	PREDICTED: uncharacterized protein LOC413627 ( <i>Apis mellifera</i> )	XP_016768806.1 PBC25613.1	342 236	4 3	0.014	-1.28	-1.25	
62	* Regucalcin [ <i>Apis cerana cerana</i> ] Unidentified				0.042	-1.24	-1.27	
63	PREDICTED: neutral alpha-glucosidase AB isoform X2 ( <i>Apis mellifera</i> )	XP_016772970.1	617	6	0.29	-2.04		
64	Unidentified				0.0051		-1.31	
65	PREDICTED: DE-cadherin isoform X2 ( <i>Apis cerana</i> )	XP_016916844.1	252	3	0.0086		-1.32	
66	Unidentified				0.0080	-1.43	-1.42	
67	PREDICTED: fibrillin-1-like, partial ( <i>Apis mellifera</i> )	XP_016773242.1	176	2	0.047		-1.43	
68	Odorant-binding protein 14 precursor ( <i>Apis mellifera</i> )	NP_001035313.1	248	3	0.0066	-1.37	-1.47	
69	PREDICTED: uncharacterized protein LOC100576902 ( <i>Apis mellifera</i> )	XP_003249902.2	205	3	0.080		-1.49	
70	Unidentified				0.044	-1.49	-1.50	
71	Odorant-binding protein 14 precursor ( <i>Apis mellifera</i> )	NP_001035313.1	530	6	0.0023	-1.39	-1.53	
72	Odorant-binding protein 14 precursor ( <i>Apis mellifera</i> )	NP_001035313.1	401	5	0.033		-1.56	

<sup>1</sup> Ratio V1 vs Control - a positive ratio denotes proteins more abundant after *Varroa* infestation and a negative ratio denotes proteins more abundant in uninfected honey bees. Ratio V2-3 vs Control - a positive ratio denotes proteins more abundant after *Varroa* infestation and a negative ratio denotes proteins more abundant in uninfected honey bees. Ratio V2-3 vs V1 - a positive ratio denotes proteins more abundant after infestation with two to three *Varroa* mother mites infestation and a negative ratio denotes proteins more abundant after one *Varroa* mother mite infestation

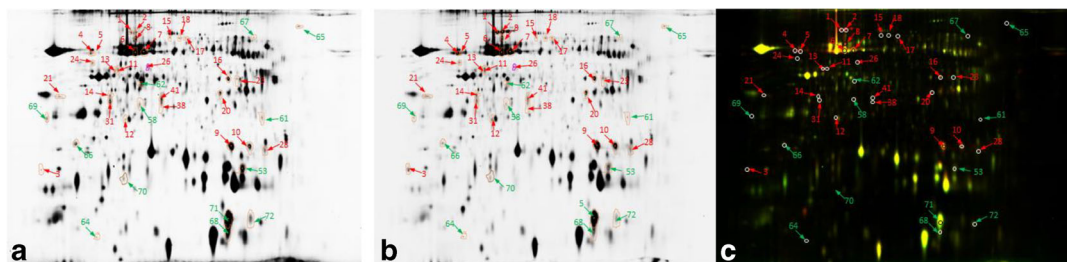


**Figure 2.** Two-dimensional difference gel electrophoresis (2D-DIGE) analysis of honey bee haemolymph proteins after infestation with two/three *Varroa* mother mites. **a** Single-channel image of proteins from control haemolymph. **b** Single-channel image of proteins from haemolymph after two/three *Varroa* mother mite infestation. **c** Overlay of Cy3 and Cy5 channel images according to haemolymph arrangement presented in Supplementary Table 1 for gel no. 4. Numbered protein spots (red) correspond to the proteins identified from 2D-DIGE that are more abundant after *Varroa* infestation and (green) indicate the identified spots that are more abundant in uninfected honey bees. Results of spot identification are presented in Table 1. **a, b** Originated directly from Biological Variation Analysis workspace of DeCyder Differential Analysis Software. **c** Originated from Image Quant TL; the differentiated proteins were marked manually in order to improve spot marking.

(1999) which indicated that not all *Varroa* mites act as vectors of DWV.

#### 4.2. Proteins characteristic for metamorphosis

Hexamerin 110 (BAI82214.1), cuticular protein precursor (NP\_001167611.1) and hexamerin (ABR45905.1; ABR45904.1) showed the largest

increase after *Varroa* infection (from +4.84 to +2.57). Hexamerins are storage proteins with primordial functions in the construction and differentiation of adult tissues during insect metamorphosis (Martins and Bitondi 2012). They are synthesised in large amounts by the larval fat cells during the larval growth phase and are secreted into the haemolymph where they accumulate. Following the larval-to-pupal moult, these

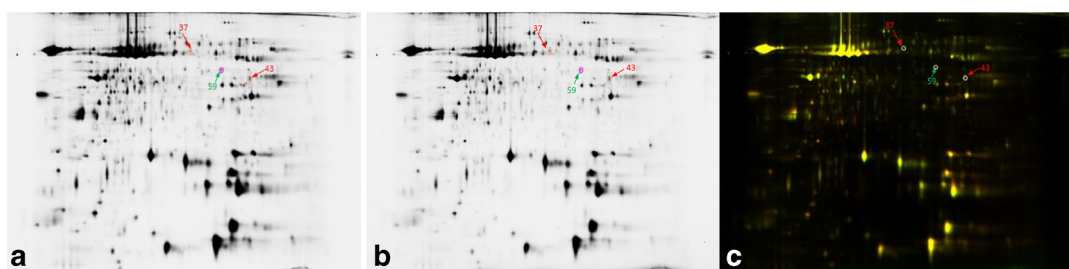


**Figure 3.** Two-dimensional difference gel electrophoresis (2D-DIGE) analysis of haemolymph proteins of honey bees infested after infestation with two to three *Varroa* mother mites in comparison to infestation with one *Varroa* mother mite. **a** Single-channel image of proteins from haemolymph after one *Varroa* mother mite infestation. **b** Single-channel image of proteins from haemolymph after infestation with two to three *Varroa* mother mites. **c** Overlay of Cy3 and Cy5 channel images according to haemolymph arrangement presented in Supplementary Table 1 for gel no. 3. Numbered protein spots (red) correspond to the proteins identified from 2D-DIGE that are more abundant after infestation with two to three *Varroa* mother mites and (green) indicate the identified spots that are more abundant after one *Varroa* mother mite infestation. Results of spots identification are presented in Table 1. **a, b** Originated directly from Biological Variation Analysis workspace of DeCyder Differential Analysis Software. **c** Originated from Image Quant TL; the differentiated proteins were marked manually in order to improve spot marking.

**Table II.** List of differentially expressed proteins in haemolymph of honey bees after infestation with *Varroa* mother mites reported according to the ratio values [from the highest ratio (+ 4.84) down to the highest decreased ratio (– 2.05)] for the three sets of data (V1 vs control; V2–3 vs control; V2–3 vs V1)

Pos.	Protein name (organism)	Ratio <sup>1</sup>		
		V1 vs control	V2–3 vs control	V2–3 vs V1
1	Hexamerin 110 ( <i>Apis mellifera</i> )		4.84	
2	Hexamerin 110 ( <i>Apis mellifera</i> )		4.71	
3	Cuticular protein precursor ( <i>Apis mellifera</i> )		3.60	
4	Hexamerin ( <i>Apis mellifera</i> )		3.25	
5	Unidentified		3.01	
6	Hexamerin ( <i>Apis mellifera</i> )		2.62	
2	Hexamerin 110 ( <i>Apis mellifera</i> )	2.57		
10	Short-chain dehydrogenase/reductase ( <i>Apis mellifera</i> )	2.35		
9	PREDICTED: dehydrogenase/reductase SDR family member 11-like ( <i>Apis dorsata</i> )	2.27		
7	Hexamerin 70a precursor ( <i>Apis mellifera</i> )		2.26	
8	Hexamerin 70a precursor ( <i>Apis mellifera</i> )		2.22	
23	Polyprotein, partial ( <i>Deformed Wing Virus</i> )	2.21		
11	PREDICTED: PTS-dependent dihydroxyacetone kinase, dihydroxyacetone-binding subunit DhaK-like ( <i>Apis mellifera</i> )	2.19		
16	PREDICTED: retinal dehydrogenase 1 ( <i>Apis mellifera</i> )	2.17		
1	Hexamerin 110 ( <i>Apis mellifera</i> )	2.15		
19	PREDICTED: beta-ureidopropionase ( <i>Apis mellifera</i> )	2.10		
4	hexamerin ( <i>Apis mellifera</i> )	2.08		
13	PREDICTED: PTS-dependent dihydroxyacetone kinase, dihydroxyacetone-binding subunit DhaK-like ( <i>Apis mellifera</i> )	2.06		
25	PREDICTED: retinal dehydrogenase 1 ( <i>Apis mellifera</i> )	2.04		
8	Hexamerin 70a precursor ( <i>Apis mellifera</i> )	2.01		
12	PREDICTED: sorbitol dehydrogenase-like ( <i>Apis mellifera</i> )	1.97		
14	PREDICTED: uncharacterized oxidoreductase YrbE-like ( <i>Apis mellifera</i> )	1.90		
17	PREDICTED: cytosolic 10-formyltetrahydrofolate dehydrogenase ( <i>Apis mellifera</i> )	1.90		
22	Unidentified	1.90		
9	PREDICTED: dehydrogenase/reductase SDR family member 11-like ( <i>Apis dorsata</i> )		1.90	
7	Hexamerin 70a precursor ( <i>Apis mellifera</i> )	1.89		
6	Hexamerin ( <i>Apis mellifera</i> )	1.87		
39	PREDICTED: fructose-bisphosphate aldolase ( <i>Apis mellifera</i> )	1.85		
10	Short-chain dehydrogenase/reductase ( <i>Apis mellifera</i> )		1.83	
11	PREDICTED: PTS-dependent dihydroxyacetone kinase, dihydroxyacetone-binding subunit DhaK-like ( <i>Apis mellifera</i> )		1.81	
12	PREDICTED: sorbitol dehydrogenase-like ( <i>Apis mellifera</i> )		1.78	
13	PREDICTED: PTS-dependent dihydroxyacetone kinase, dihydroxyacetone-binding subunit DhaK-like ( <i>Apis mellifera</i> )		1.77	
5	Unidentified	1.76		
15	PREDICTED: glycogen phosphorylase ( <i>Apis mellifera</i> )	1.76		

**Table II** (continued)

Pos.	Protein name (organism)	Ratio <sup>1</sup>		
		V1 vs control	V2–3 vs control	V2–3 vs V1
24	PREDICTED: transketolase-like protein 2 isoform X2 ( <i>Apis mellifera</i> )	1.74		
14	PREDICTED: uncharacterized oxidoreductase YrBE-like ( <i>Apis mellifera</i> )		1.74	
20	PREDICTED: beta-ureidopropionase ( <i>Apis mellifera</i> )	1.68		
15	PREDICTED: glycogen phosphorylase ( <i>Apis mellifera</i> )		1.66	
27	PREDICTED: 6-phosphogluconate dehydrogenase, de lating ( <i>Apis mellifera</i> )	1.65		
16	PREDICTED: retinal dehydrogenase 1 ( <i>Apis mellifera</i> )		1.65	
17	PREDICTED: cytosolic 10-formyltetrahydrofolate dehydrogenase ( <i>Apis mellifera</i> )		1.62	
29	PREDICTED: beta-ureidopropionase ( <i>Apis mellifera</i> )	1.61		
18	PREDICTED: cytosolic 10-formyltetrahydrofolate dehydrogenase ( <i>Apis mellifera</i> )	1.58		
30	PREDICTED: phosphoglucomutase isoform X1 ( <i>Apis mellifera</i> )	1.57		
18	PREDICTED: cytosolic 10-formyltetrahydrofolate dehydrogenase ( <i>Apis mellifera</i> )		1.55	
26	PREDICTED: T-complex protein 1 subunit zeta ( <i>Apis florea</i> )	1.53		
20	PREDICTED: beta-ureidopropionase ( <i>Apis mellifera</i> )		1.53	
21	PREDICTED: 3-ketoacyl-CoA thiolase, mitochondrial ( <i>Apis mellifera</i> )		1.51	
35	PREDICTED: glutathione S-transferase S1 isoform X1 ( <i>Apis mellifera</i> )	1.50		
32	PREDICTED: isocitrate dehydrogenase (NADP) cytoplasmic ( <i>Apis mellifera</i> )	1.48		
23	Polyprotein, partial ( <i>Deformed Wing Virus</i> )		1.48	
36	Peroxiredoxin-like protein ( <i>Apis mellifera</i> )	1.45		
24	PREDICTED: transketolase-like protein 2 isoform X2 ( <i>Apis mellifera</i> )		1.45	
26	PREDICTED: T-complex protein 1 subunit zeta ( <i>Apis florea</i> )		1.38	
33	Carboxylesterase ( <i>Apis mellifera</i> )	1.37		
34	Hexamerin ( <i>Apis mellifera</i> )	1.36		
40	PREDICTED: glucose-6-phosphates isomerase ( <i>Apis mellifera</i> )	1.31		
28	Unidentified		1.31	
31	PREDICTED: fructose-bisphosphate aldolase ( <i>Apis mellifera</i> )		1.26	
37	PREDICTED: beta-glucuronidase ( <i>Apis mellifera</i> )			1.24
43	PREDICTED: serine protease easter ( <i>Apis mellifera</i> )			1.19
38	PREDICTED: aldose 1-epimerase isoform X1 ( <i>Apis mellifera</i> )		1.14	
41	PREDICTED: aldose 1-epimerase isoform X2 ( <i>Apis mellifera</i> )		1.13	
53	Unidentified		– 1.14	
50	PREDICTED: insulin-like growth factor-binding protein complex acid labile subunit ( <i>Apis mellifera</i> )	– 1.19		
48	Unidentified	– 1.19		
46	PREDICTED: circadian clock-controlled protein ( <i>Apis mellifera</i> )	– 1.21		
51	PREDICTED: putative cysteine proteinase CG12163 isoform X2 ( <i>Apis mellifera</i> )	– 1.22		
44	PREDICTED: membrane metallo-endopeptidase-like 1 isoform X2 ( <i>Apis mellifera</i> )	– 1.22		

**Table II** (continued)

Pos.	Protein name (organism)	Ratio <sup>1</sup>		
		V1 vs control	V2-3 vs control	V2-3 vs V1
58	Unidentified		- 1.22	
57	PREDICTED: general odorant-binding protein 56d-like ( <i>Apis cerana</i> )	- 1.24		
62	Unidentified	- 1.24		
61	PREDICTED: uncharacterized protein LOC413627 ( <i>Apis mellifera</i> )		- 1.25	
	Regucalcin ( <i>Apis cerana cerana</i> )			
62	Unidentified		- 1.27	
54	PREDICTED: putative defense protein 3 ( <i>Apis mellifera</i> )	- 1.28		
61	PREDICTED: uncharacterized protein LOC413627 ( <i>Apis mellifera</i> )	- 1.28		
	Regucalcin ( <i>Apis cerana cerana</i> )			
45	Unidentified	- 1.30		
64	Unidentified		- 1.31	
55	PREDICTED: LOW QUALITY PROTEIN: apolipoporphins ( <i>Apis mellifera</i> )	- 1.32		
65	PREDICTED: DE-cadherin isoform X2 ( <i>Apis mellifera</i> )		- 1.32	
56	Unidentified	- 1.33		
68	Odorant-binding protein 14 precursor ( <i>Apis mellifera</i> )	- 1.37		
49	PREDICTED: chitinase-like protein Idgf4 isoform X1 ( <i>Apis mellifera</i> )	- 1.37		
71	Odorant-binding protein 14 precursor ( <i>Apis mellifera</i> )	- 1.39		
52	PREDICTED: chitinase-like protein Idgf4 isoform X2 ( <i>Apis mellifera</i> )	- 1.40		
42	PREDICTED: chitobiosyldiphosphodolichol beta-mannoosyltransferase-like ( <i>Apis mellifera</i> )	- 1.41		
47	Unidentified	- 1.42		
66	Unidentified	- 1.43		
66	Unidentified		- 1.42	
67	PREDICTED: fibrillin-1-like, partial ( <i>Apis mellifera</i> )		- 1.43	
68	Odorant-binding protein 14 precursor ( <i>Apis mellifera</i> )		- 1.47	
70	Unidentified	- 1.49		
69	PREDICTED: uncharacterized protein LOC100576902 ( <i>Apis mellifera</i> )		- 1.49	
70	Unidentified		- 1.50	
59	PREDICTED: protein disulfide-isomerase A3 ( <i>Apis mellifera</i> )			- 1.51
71	Odorant-binding protein 14 precursor ( <i>Apis mellifera</i> )		- 1.53	
72	Odorant-binding protein 14 precursor ( <i>Apis mellifera</i> )		- 1.56	
63	PREDICTED: neutral alpha-glucosidase AB isoform X2 ( <i>Apis mellifera</i> )	- 2.04		
60	PREDICTED: neutral alpha-glucosidase AB isoform X1 ( <i>Apis mellifera</i> )	- 2.05		

<sup>1</sup> Ratio V1 vs Control - a positive ratio denotes proteins more abundant after *Varroa* infestation and a negative ratio denotes proteins more abundant in uninfected honey bees. Ratio V2-3 vs Control - a positive ratio denotes proteins more abundant after *Varroa* infestation and a negative ratio denotes proteins more abundant in uninfected honey bees. Ratio V2-3 vs V1 - a positive ratio denotes proteins more abundant after infestation with two to three *Varroa* mother mites infestation and a negative ratio denotes proteins more abundant after one *Varroa* mother mite infestation

proteins are sequestered from haemolymph by the fat body cells, via endocytosis mediated by membrane receptors (Burmester and Scheller 1999),

and stored in the cytoplasm in the form of granules (Levenbook 1985) to act solely as storage proteins that provide amino acids and energy

**Table III.** Participation of differentially expressed haemolymph proteins in different pathways after *Varroa* infestation according to GO classification (molecular function) and to published knowledge

Protein pathways	Spot number	Proteins	Ratio <sup>1</sup>		
			V1 vs control	V2–3 vs control	V2–3 vs V1
<b>Carbohydrate metabolism</b>					
Glycolysis/ gluconeogenesis	31, 39	PREDICTED: fructose-bisphosphate aldolase	1.85	1.26	#
	40	PREDICTED: glucose-6-phosphate isomerase	1.31	#	#
	30	PREDICTED: phosphoglucomutase isoform X1	1.57	#	#
	11, 13	PREDICTED: PTS-dependent dihydroxyacetone kinase, dihydroxyacetone-binding subunit DhaK-like	2.19; 2.06	1.81; 1.77	#
	15	PREDICTED: glycogen phosphorylase	1.76	1.66	#
Pentose phosphate pathway	27	PREDICTED: 6-phosphogluconate dehydrogenase, decarboxylating	1.65	#	#
	24	PREDICTED: transketolase-like protein 2 isoform X2	1.74	1.45	#
	30	PREDICTED: phosphoglucomutase isoform X1	1.57	#	#
	37	PREDICTED: beta-glucuronidase	#	#	1.24
	16, 25	PREDICTED: retinal dehydrogenase 1	2.17; 2.04	1.65	#
	15	PREDICTED: glycogen phosphorylase	1.76	1.66	#
Glycogen synthesis	30	PREDICTED: phosphoglucomutase isoform X1	1.57	#	#
TCA cycle	32	PREDICTED: isocitrate dehydrogenase [NADP] cytoplasmic	1.48	#	#
Sucrose metabolism	12	PREDICTED: sorbitol dehydrogenase-like Du Rand et al. (2015), Kunieda et al. (2006), Erban et al. (2014)	1.97	1.78	#
<b>Detoxification and oxidative stress response</b>					
Antioxidant activity	36	Peroxiredoxin-like protein	1.45	#	#
	35	PREDICTED: glutathione S-transferase S1 isoform X1	1.50	#	#
Chaperone proteins	26	PREDICTED: LOW QUALITY PROTEIN: T-complex protein 1 subunit zeta	1.53	1.38	#
Toxin detoxification	33	Carboxylesterase	1.37	#	#
	35	PREDICTED: glutathione S-transferase S1 isoform X1 Du Rand et al. (2015), Erban et al. (2016)	1.50	#	#
<b>Chemosensing</b>					
Olfactory system	68, 71	Odorant-binding protein 14 precursor	-1.37; -1.39	-1.47; -1.53	#
	72	Odorant-binding protein 14 precursor	#	-1.56	#
	57	PREDICTED: general odorant-binding protein 56d-like	-1.24	#	#

**Table III** (continued)

Protein pathways	Spot number	Proteins	Ratio <sup>1</sup>		
			V1 vs control	V2–3 vs control	V2–3 vs V1
		Du Rand et al. (2015), Zhu et al. (2016), Erban et al. (2014, 2016)			
Immunity					
Immune-responsive proteins	55	PREDICTED: LOW QUALITY PROTEIN: apolipoporphins	– 1.32	#	#
Defense protein family (innate immune response, defense response to bacterium)	54	PREDICTED: putative defense protein 3	– 1.28	#	#
		Gätschenberger et al. (2013), Erban et al. (2014, 2016)			
Nutrient reservoir activity	4, 6	Hexamerin	2.08; 1.87	3.25; 2.62	#
	34	Hexamerin	1.36	#	#
	1, 2	Hexamerin 110	2.15; 2.57	4.84; 4.71	#
	7, 8	Hexamerin 70a precursor	1.89; 2.01	2.26; 2.22	#
		Burmester and Scheller (1999), Martins and Bitondi (2012), Cunha et al. (2005), Erban et al. (2014)			
Oxidoreductase activity	10	Short-chain dehydrogenase/reductase	2.35	1.83	#
	14	PREDICTED: uncharacterized oxidoreductase YrBE-like	1.90	1.74	#
	12	PREDICTED: sorbitol dehydrogenase-like	1.97	1.78	#
	17, 18	PREDICTED: cytosolic 10-formyltetrahydrofolate dehydrogenase	1.90; 1.58	1.62; 1.55	#
		Erban et al. (2014)			
Metabolic pathways	51	PREDICTED: putative cysteine proteinase CG12163 isoform X2	– 1.22	#	#
	44	PREDICTED: membrane metallo-endopeptidase-like 1 isoform X2	– 1.22	#	#
Lipid metabolism	21	3-ketoacyl-CoA thiolase, mitochondrial	#	1.51	
		Erban et al. (2014)			
Genetic information processing (translation, transcription, protein processing and folding)	60	PREDICTED: neutral alpha-glucosidase AB isoform X1	– 2.05	#	#
	63	PREDICTED: neutral alpha-glucosidase AB isoform X2	– 2.04	#	#
Protein processing in ER	59	Protein disulfide-isomerase A3	#	#	– 1.51
		Du Rand et al. (2015)			
Branched chain amino acid metabolism	16, 25	Retinal dehydrogenase 1-like isoform 1	2.17; 2.04	1.65; #	#

**Table III** (continued)

Protein pathways	Spot number	Proteins	Ratio <sup>1</sup>		
			V1 vs control	V2-3 vs control	V2-3 vs V1
(valine, leucine and isoleucine degradation)	21	3-Ketoacyl-CoA thiolase, mitochondrial Du Rand et al. (2015)	#	1.51	#
Protein not associated with predicted pathways	19, 20	PREDICTED: beta-ureidopropionase	2.10; 1.68	#, 1.53	#
	29	PREDICTED: beta-ureidopropionase	1.61	#	#
	43	PREDICTED: serine protease easter	#	#	1.19
	61	Regucalcin	- 1.28	- 1.25	#
	46	PREDICTED: circadian clock-controlled protein	- 1.21	#	#
	65	PREDICTED: DE-cadherin isoform X2	#	- 1.32	#
	67	PREDICTED: fibrillin-1-like, partial	#	- 1.43	#
	69	PREDICTED: uncharacterized protein LOC100576902	#	- 1.49	#
	50	PREDICTED: insulin-like growth factor-binding protein complex acid labile subunit	- 1.19	#	#
	42	PREDICTED: chitobiosyldiphosphodichol beta-mannosyltransferase-like	- 1.24 - 1.41	# #	# #
	49, 52	PREDICTED: chitinase-like protein Idgf4 isoform X2	- 1.37; - 1.40	#	#
	38	PREDICTED: aldose 1-epimerase isoform X1	#	1.14	#
	41	PREDICTED: aldose 1-epimerase isoform X2	#	1.13	#
	3	cuticular protein precursor	#	3.60	#
9	PREDICTED: dehydrogenase/reductase SDR family member 11-like	2.27	1.90	#	

<sup>1</sup> Ratio V1 vs Control - a positive ratio denotes proteins more abundant after *Varroa* infestation and a negative ratio denotes proteins more abundant in uninfected honey bees. Ratio V2-3 vs Control - a positive ratio denotes proteins more abundant after *Varroa* infestation and a negative ratio denotes proteins more abundant in uninfected honey bees. Ratio V2-3 vs V1 - a positive ratio denotes proteins more abundant after infestation with two to three *Varroa* mother mites infestation and a negative ratio denotes proteins more abundant after one *Varroa* mother mite infestation; # the lack of differences

during non-feeding periods (Zakharkin et al. 2001; Jamroz et al. 1996). Therefore, the level of hexamerins must be maintained at some level to play a role as storage proteins.

Four hexamerin proteins, hexamerin70a, hexamerin 70b, hexamerin 70c and hexamerin 110, were identified in different stages of the honey bee (Martins et al. 2010, 2011; Erban et al. 2016). At the time of emergence, 70b, 70c and 110 disappeared, and 70a appeared constant (Erban et al. 2016). Thus, hexamerin 70a in

haemolymph appears to play a different role to hexamerin 70b, 70c and 110. According to Erban et al. (2016) at the time of emergence, Hex70a is not used primarily as a storage protein but has a transport function; hexamerins may transport hormones such as juvenile hormone (Braun and Wyatt 1996). In our opinion, it is interesting that the loss of haemolymph during *Varroa* parasitism was not accompanied by the loss of hexamerin in honey bee haemolymph. Perhaps the increased secretion of hexamerins to the



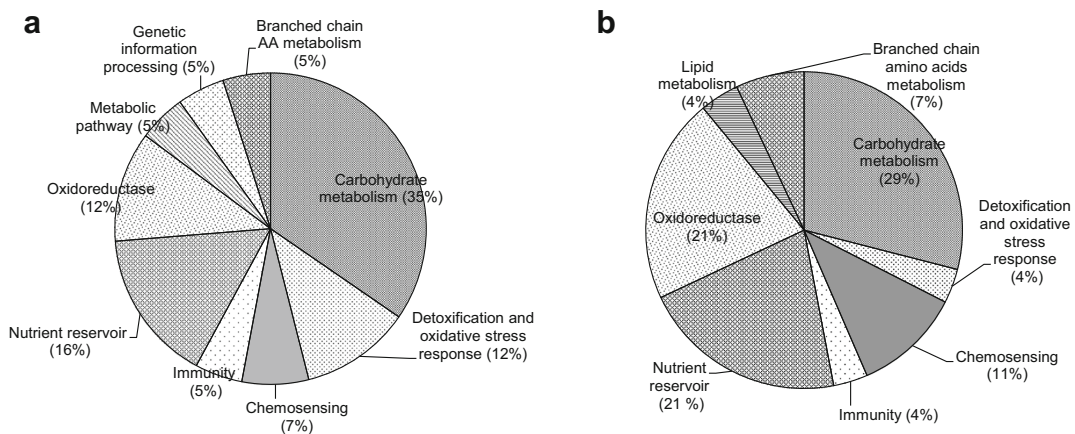


**Figure 4.** The classification of the honey bee haemolymph proteins after infestation with one (a) and two–three (b) *Varroa* mother mites according to GO classification (molecular function).

haemolymph is a part of the mechanism aimed to compensate for the loss of storage proteins in honey bee haemolymph due to *Varroa* infestation. Besides acting as a storage protein, hexamerin participates in tissue development during insect metamorphosis (Martins and Bitondi 2012). An increased level of cuticular protein precursor can also suggest that metamorphic and imaginal moulting events are disrupted after

*Varroa* infestation. For this reason, it can be assumed that maintaining high levels of hexamerin and cuticular protein under conditions of *Varroa* infestation is also important for the protection of normally differentiated tissue and the exoskeleton during metamorphosis. The largest increased ratio observed in our study for hexamerins and cuticular protein after *Varroa* infestation indicated that the reported proteins may be crucial for the

**Table IV.** Results from Ingenuity Pathway Analysis of honey bee haemolymph proteins after infestation with *Varroa* mother mites

Ingenuity canonical pathways	Infestation with 1 <i>Varroa</i> <i>p</i> value	Infestation with 2–3 <i>Varroa</i> <i>p</i> value	Gene impacted
Glucose and glucose 1-phosphate degradation	9.30E-05	1.35E-04	PGM1, RGN
Pentose phosphate pathway	9.30E-05	1.35E-04	PGD, TKT
Glycogen degradation II	1.32E-04	1.92E-04	PYGM, PGM1
Glycogen degradation III	1.77E-04	2.58E-04	PYGM, PGM1
Molecular and cellular function	<i>p</i> value range		
Carbohydrate metabolism	4.29E-02–5.89E-11	3.77E-02–1.88E-10	ALDOA, CHIT1, GPI, IDH1, PGD, PGM1, PRDX6, PYGM, RGN, SORD, TKT, GANAB

PGM1—phosphoglucomutase isoform X1 (30); RGN—regucalcin (61); PGD—6-phosphogluconate dehydrogenase (27); TKT—transketolase-like protein 2 (24); PYGM—glycogen phosphorylase (15); ALDOA—fructose-bisphosphate aldolase (31); CHIT1—chitinase-like protein (49, 52); GPI—glucose-6-phosphate isomerase (40); IDH1—iscitrate dehydrogenase (NADP) cytoplasmic (32); PRDX6—peroxiredoxin-like protein (36); SORD—sorbitol dehydrogenase-like (12); GANAB—neutral alpha-glucosidase AB (60, 63)

response of honey bees to *Varroa* infestation and, for this reason, may be potential biomarkers of *Varroa* infestation.

#### 4.3. The neutral alpha-glucosidase AB and protein disulfide-isomerase A3

The neutral alpha-glucosidase AB isoform X1, isoform X2 (XP\_016772970.1) and protein disulfide-isomerase A3 (XP\_623282.1) were proteins that decreased the most after infection with *Varroa* mite (from  $-2.05$  to  $-1.51$ ). Neutral alpha-glucosidases AB are involved in sugar metabolism and potentially in detoxification in insects (Li et al. 2016). Protein disulfide-isomerase catalyses the rearrangement of  $-S-S-$  bonds in proteins and participates in cell redox homeostasis. These reported proteins were classified as proteins processing in the endoplasmic reticulum by Du Rand et al. (2015) that responded to nicotine exposure.

#### 4.4. Olfaction-odorant-binding proteins

This study strongly suggests disruption of honey bee olfaction after infection with *Varroa* mites. Odorant-binding protein 14 precursors (NP\_001035313.1; OBPs) showed one of the most significant decreases after *Varroa* infection. Based on the results of a previous study, OBPs are known to play a role in chemosensing and chemical communication in insects (Zhu et al. 2016). OBPs are involved in carrying hydrophobic odors and pheromones from the external environment to the membrane of chemosensory neurons across the aqueous lymph of chemosensilla (Vogt 2003; Pelosi et al. 2006; Leal 2013). Numerous chemical signals crucial for the function in the society and behaviour of forager bees, such as longer flight duration and homing ability, are affected by *Varroa* (Kralj and Fuchs 2006). Interestingly, *Varroa*-sensitive hygiene honey bee colonies were characterised by a higher abundance of OBPs in the mushroom body and antenna (Hu et al. 2016), suggesting a crucial role of the reported proteins in defence against *Varroa*. In summary, our results suggest that infestation with *Varroa* impairs the olfactory system of honey

bees and could lead to disruption of chemosensing and chemical communication.

#### 4.5. Protein of carbohydrate and glucose metabolism

Here, we demonstrated the up-regulation of proteins participating in the glycolysis, gluconeogenesis and glycogen synthesis after *Varroa* infestation. Moreover, six up-regulated proteins were linked together by IPA with a functional network for glucose synthesis (Figure 5). We believe that these results suggest that the higher abundance of enzymes involved in glucose metabolism reflects a decrease in carbohydrate concentrations, as reported by Bowen-Walker and Gunn (2001) for adult worker honey bee abdomen after *Varroa* infestation. Perhaps, the induction of enzymes participating in glycolysis/gluconeogenesis and glycogen synthesis is part of the mechanism aimed to compensate glucose losses from honey bee haemolymph due to *Varroa* infestation.

#### 4.6. Protein of detoxification and oxidative stress response

The three proteins, peroxiredoxin-like protein (NP\_001164444.1), glutathione S-transferase S1 isoform X1 (XP\_016772844.1) and T-complex protein 1 subunit zeta (XP\_012349557.1), were present at increased levels in the *Varroa*-infected bee samples. Moreover, peroxiredoxin-like protein and glutathione S-transferase S1 are also involved in the response to oxidative stress (Du Rand et al. 2015; Erban et al. 2016) and T-complex proteins are classified as chaperone proteins (Du Rand et al. 2015). In our opinion, the increased level of the latter protein suggests an increase in the amount of incorrectly folded proteins in *Varroa*-infected bees. Finally, another protein, carboxylesterase (NP\_001136081.1), was also found at higher levels in *Varroa*-infected bee samples; together with glutathione S-transferase, this protein is involved in the detoxification of low doses of insecticides (Badawy et al. 2015). In summary, the results suggest that up-regulation of haemolymph proteins participating in detoxification and response to oxidative stress might be part

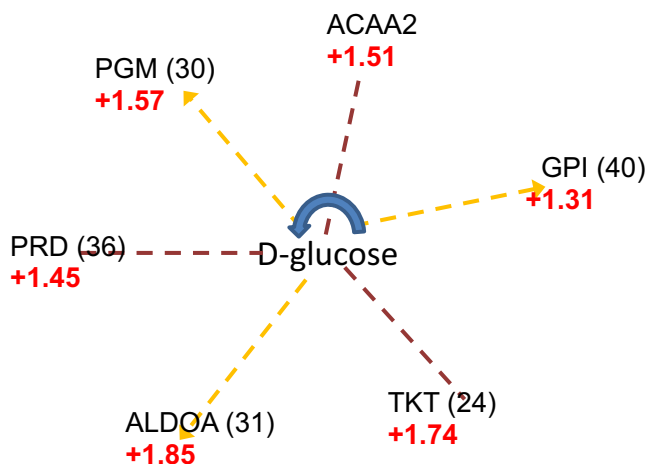


**Figure 5.** Haemolymph protein network associated with *Varroa* infestation. The network was done using Ingenuity Pathway Analysis. Red numbers indicate the level of abundance after *Varroa* infestation. ACAA2—3-ketoacyl-CoA thiolase, mitochondrial; ALDOA—fructose-bisphosphate aldolase; GPI—glucose-6-phosphate isomerase; PGM—phosphoglucomutase isoform X1; PRD—peroxiredoxin-like protein; TKT—transketolase-like protein 2 isoform X2. Spot numbers in brackets are presented according to Table 1.

of the mechanism characteristic of the response of honey bees to the pathogenic action of *Varroa*.

#### 4.7. Immune-related proteins

We observed down-regulation of two immune-related proteins [apolipoporphins (XP\_016768851.1) and putative defense protein 3 (XP\_003249096.1)] in the haemolymph after infestation with one *Varroa* mite. Interestingly, the apparent suppression of immune-related proteins was not observed when honey bees were faced with higher mite loads (two to three *Varroa* mites per pupa). The lack of strong immune system responses after *Varroa* infestation can be explained by host immunosuppression by the combined action of *Varroa* and DWV. Honey bees with increasing DWV loads have reduced immunocompetence at both the humoral and the cellular levels (Di Prisco et al. 2016; Ryabov et al. 2014). Further studies should aim to understand the molecular mechanism of immune responses in relation to the degree of *Varroa* infestation.

The results of this study indicated disturbance in the immune response involving high molecular weight protein due to *Varroa* infestation. However, in our study, we did not identify any known antimicrobial peptides (AMPs) in haemolymph of infested honey bees (Randolt et al. 2008), such as

apidaecins, abaecin and defensins. The lack of AMP identification can be explained by limitations in 2DE detection of denatured proteins (size range of 10–200 kDa; Molloy and McDowell 2005). Randolt et al. (2008) used Tricine–SDS-PAGE (separation range from 1 to 100 kDa) and clearly showed that AMPs in honey bee haemolymph have a molecular mass below 10 kDa. For this reason, AMPs could not be identified under the conditions of 2D-DIGE. Further studies should focus on more complete characterisation of the immune response, including low molecular weight AMPs, after *Varroa* infestation.

Phenoloxidase is an important part of defence against intruding microorganisms and parasites, including *Varroa* (Koleoglu et al. 2018), wound healing and cuticle pigmentation (Zufelato et al. 2004; Binggeli et al. 2014). However, in our study, we did not demonstrate differences in phenoloxidase abundance in honey bee haemolymph after *Varroa* infestation. The molecular weight of phenoloxidase is 70 kDa (Zufelato et al. 2004). On a 2DE image presented by Erban et al. (2016), phenoloxidase was detected in an area of high molecular weight proteins near to hexamerins—one of the most abundant proteins in 1-day-old honey bee haemolymph (this study).

To our knowledge, among the published 2DE studies of haemolymph of newly emerged honey bees, only one study reported detection of phenoloxidase (Erban et al. 2016); phenoloxidase was not detected in studies by Feng et al. (2014) and Erban et al. (2014). Due to low relative abundance, prophenol oxidase may be masked by the presence of more abundant proteins with similar physicochemical characteristics, such as hexamerins, and therefore, we were not able to detect this protein under the conditions of 2D-DIGE.

#### 4.8. Oxidoreductases

We observed up-regulation of five enzymes assigned to oxidoreductase activity after *Varroa* infestation. The activity of several oxidoreductases has been demonstrated in the haemolymph of honey bees (Tripathi and Dixon 1969; Gilliam and Jackson 1972), and they play diverse functions in the metabolism (Erban et al. 2014). The latter authors identified three of five oxidoreductases found in our study: short-chain dehydrogenase/reductase (NP\_001011620.1; SDR), sorbitol dehydrogenase-like (XP\_392401.3; SDH) and oxidoreductase YrBE (XP\_624408.2) and classified them as secondary metabolites of biosynthesis, transport and catabolism (Erban et al. 2014). The SDH is an enzyme involved in the polyol pathway and catalyses the conversion of sorbitol to fructose (Marchler-Bauer et al. 2013). An increased level of SDH after *Varroa* infestation agrees with the up-regulation of enzymes involved in glucose metabolism (see above). Moreover, an increased level of oxidoreductase YrBE, together with SDH, suggests a function in energy production and conversion (Erban et al. 2014). In a previous study, SDR was a target of ecdysone (an ecdysteroid, produced by the prothoracic gland, that controls moulting in the larva and pupa) response during honey bee caste development (Guidugli et al. 2004). Summing up, our results suggest that the increased abundance of oxidoreductases after *Varroa* infestation may be related to diverse metabolic and physiological functions such as energy production and development.

#### 4.9. Proteins of branched chain amino acid metabolism and lipid metabolism

As mentioned above, the biochemical and physiological pathways most affected (up- and down-regulated) due to *Varroa* infestation were represented by several proteins; in addition, we observed up-regulation in a few proteins involved in branched chain amino acid metabolism (BCAA) and lipid metabolism. The BBAAs are the most hydrophobic of the amino acids and play crucial roles in determining the structures of globular proteins (Brosnan and Brosnan 2006). This agrees with the increases of T-complex protein 1 subunit zeta (XP\_012349557.1) involved in protein stabilisation. An increased level of 3-ketoacyl-CoA thiolase (XP\_391843.1), involved in lipid metabolism, may be associated with an increased synthesis of hexamerin by the larval fat body in response to *Varroa* infestation (Telfer and Kunkel 1991). In addition, we observed down-regulation for proteins involved in metabolic pathways and genetic information processing such as translation, transcription, protein processing and folding. This suggests that *Varroa* infestation has a negative effect both on the expression of genetic information and the maintenance of an optimal protein structure.

Lipid transport involving vitellogenin (Vg) is the most significantly enriched biological process in the foundress (reproductive female) and in young mites (McAfee et al. 2017), suggesting that honey bee Vg may be altered by *Varroa* infestation. However, in our study, no alteration of Vg was found in 1-day-old honey bee haemolymph after *Varroa* infestation. The reason for the lack of Vg alteration in our study may result from low Vg concentrations in the haemolymph of summer bees. This suggestion is supported by the results of proteomic studies of summer (Bogaerts et al. 2009) and winter honey bee haemolymph (Erban et al. 2013) where a negligible level of Vg was identified in summer bees in comparison to an abundant level of Vg in the haemolymph of winter honey bees.

#### 4.10. Proteins of other categories

In this study, we observed that changes in abundance of some proteins were restricted only

to changes in particular isoforms and/or proteoforms. Therefore, it cannot be assumed that, for example, in sum hexamerin 70a (NP\_001104234.1) changed, since the changes were visible only within two isoforms and/or proteoforms produced as a result of post-translational modification. A similar situation was observed for other proteins that changed only within a few isoforms and/or proteoforms, such as apolipoporphins (XP\_016768851.1; 1 isoform), beta-ureidopropionase (XP\_392773.3; 3 isoforms), hexamerin (ABR45904.1; ABR45905.1; 3 isoforms), hexamerin 110 (BAI82214.1; 2 isoforms) and neutral alpha-glucosidase (XP\_016772970.1; 2 isoforms). Overall, our study indicated that changes in honey bee haemolymph after *Varroa* mite infestation did not always affect all proteins, but may reflect changes in particular isoforms and/or proteoforms.

Here, we identified a few individual proteins that could not be assigned to the major protein function categories. The altered abundance of the cuticular protein precursor (NP\_001167611.1) and chitinase-like protein (XP\_016773072.1), compounds of insect cuticle layers (Zhao et al. 2017), suggests a disruption in the honey bee exoskeleton after *Varroa* infestation. The down-regulation of the circadian clock-controlled protein (XP\_001122696.1) suggests circadian behavioural rhythm disorder (Fuchikawa et al. 2017). Moreover, *Varroa* infestation can affect ATP, calcium and carbohydrate binding by changing the expression of fibrillin-1-like (XP\_016773242.1) and aldose 1-epimerase isoform Xa (XP\_016772523.1), respectively. All together, these results suggest that several physiological functions, such as morphogenesis/metamorphosis, circadian behavioural rhythm and energy metabolism, may be impaired as a consequence of *Varroa* infestation.

## 5. CONCLUSIONS

In summary, our study indicates multifactorial effects of *Varroa* infestation on honey bees, highlighting the most disrupted physiological pathways of honey bee haemolymph, such as carbohydrate metabolism, detoxification and oxidative stress response, nutrient reservoir activity, oxidoreductase activity and the olfactory system.

Immune-related proteins could not be completely identified under the conditions of 2D-DIGE in 1-day-old honey bee workers. Several physiological functions of the honey bee including energy metabolism, detoxification, chemosensing and metamorphosis may be disrupted by *Varroa*. The latter, represented by hexamerins and cuticular protein, seems to be mostly affected by *Varroa* infestation. The presence of increased levels of polyprotein of the deformed wing virus in honey bee haemolymph could be a biomarker of *Varroa* parasitism. *Varroa* infestation can be a result of host immunosuppression by the combined actions of *Varroa* and DWV. Knowledge regarding proteome changes can be the basis of further studies investigating the detailed mechanisms of honey bee responses to *Varroa* infestation.

## ACKNOWLEDGEMENTS

The authors wish to thank Halina Karol and Ewa Liszewska for technical assistance with the mass spectrometry sample preparation. The authors would like to thank the two anonymous reviewers for their valuable comments and suggestions. Raw MALDI-TOF/TOF data have been deposited to the ProteomeXchange Consortium via the PRIDE partner repository with the dataset identifier PXD012429.

## AUTHOR CONTRIBUTIONS

BB, JW and MSi participated in the design of the experiment and the haemolymph collection; MSi managed the colonies of honey bee workers for haemolymph collection; MSi and JN performed the experiment and the analysis; MSi and AC wrote the paper and participated in paper revision. All authors read and approved the final manuscript.

## FUNDING INFORMATION

This work was funded by the Institute of Animal Reproduction and Food Research and the University of Warmia and Mazury in Olsztyn.

**L'analyse protéomique 2D-DIGE révèle des changements dans le protéome de l'hémolymphe d'ouvrières âgées d'un jour (*Apis mellifera*) en réponse à une infestation par des acariens *Varroa destructor***

*Apis mellifera* / *Varroa destructor* / Hämolymphe /  
protéome / DIGE

**Eine 2D-DIGE Proteomanalyse zeigt Veränderungen  
im Hämolympf-Proteom von eintägigen Honigbienen-  
Arbeiterinnen (*Apis mellifera*) als Antwort auf einen  
Befall mit Varroamilben**

*Apis mellifera* / *Varroa destructor* / Hämolymphe /  
Proteom / DIGE

## OPEN ACCESS

This article is distributed under the terms of the Creative Commons Attribution 4.0 International License (<http://creativecommons.org/licenses/by/4.0/>), which permits unrestricted use, distribution, and reproduction in any medium, provided you give appropriate credit to the original author(s) and the source, provide a link to the Creative Commons license, and indicate if changes were made.

## REFERENCES

- Allen, M., Ball, B. (1996) The incidence and world distribution of honey bee viruses. *Bee World* **77** (3), 141–162, <https://doi.org/10.1080/0005772X.1996.11099306>
- Ararso, Z., Ma, C., Qi, Y., Feng, M., Han, B., et al. (2018) Proteome comparisons between hemolymph of two honeybee strains (*Apis mellifera ligustica*) reveal divergent molecular basis in driving hemolymph function and high royal jelly secretion. *J. Proteome Res.* **17** (1), 402–419, <https://doi.org/10.1021/acs.jproteome.7b00621>
- Badawy, M.E.I., Nasr, H.M., Rabea E.I. (2015) Toxicity and biochemical changes in the honey bee *Apis mellifera* exposed to four insecticides under laboratory conditions. *Apidologie* **46** (2), 177–193, <https://doi.org/10.1007/s13592-014-0315-0>
- Barceló-Batllori, S., Kalko, S.G., Esteban, Y., Moreno, S., Carmona, M.C., et al. (2008) Integration of DIGE and bioinformatics analyses reveals a role of the antiobesity agent tungstate in redox and energy homeostasis pathways in brown adipose tissue. *Mol. Cell Proteomics* **7** (2), 378–393, <https://doi.org/10.1074/mcp.M700198-MCP200>
- Beckett, P. (2012) The basics of 2D DIGE. *Methods Mol. Biol.* **854**, 9–19, [https://doi.org/10.1007/978-1-61779-573-2\\_2](https://doi.org/10.1007/978-1-61779-573-2_2)
- Binggeli, O., Neyen, C., Poidevin, M., Lemaitre, B. (2014) Prophenoloxidase activation is required for survival to microbial infections in *Drosophila*. *PLoS Pathog.* **10** (5), e1004067, <https://doi.org/10.1371/journal.ppat.1004067>
- Bogaerts, A., Baggerman, G., Vierstraete, E., Schoofs, L., Verleyen, P. (2009) The hemolymph proteome of the honeybee: gel-based or gel-free? *Proteomics* **9** (11), 3201–3208, <https://doi.org/10.1002/pmic.200800604>
- Borsuk, G., Ptasińska, A.A., Olszewski, K., Domaciuk, M., Krutmuang, P., et al. (2017) A new method for quick and easy hemolymph collection from *Apidae* adults. *Plos One* **12** (1), e0170487, <https://doi.org/10.1371/journal.pone.0170487>
- Bowen-Walker, P.L., Gunn, A. (2001) The effect of the ectoparasitic mite, *Varroa destructor* on adult worker honeybee (*Apis mellifera*) emergence weights, water, protein, carbohydrate, and lipid levels. *Entomol. Exp. Appl.* **101** (3), 207–217 <https://doi.org/10.1046/j.1570-7458.2001.00905.x>
- Bowen-Walker, P.L., Martin, S.J., Gunn, A. (1999) The transmission of deformed wing virus between honeybees (*Apis mellifera* L.) by the ectoparasitic mite *Varroa jacobsoni* Oud. *J. Invertebr. Pathol.* **73** (1), 101–106, <https://doi.org/10.1006/jjpa.1998.4807>
- Bradford, M. M. (1976). A rapid and sensitive method for the quantitation of microgram quantities of protein utilizing the principle of protein-dyebinding. *Anal. Biochem.* **72**, 248–254, [https://doi.org/10.1016/0003-2697\(76\)90527-3](https://doi.org/10.1016/0003-2697(76)90527-3)
- Braun, R.P., Wyatt, G.R. (1996) Sequence of the hexameric juvenile hormone-binding protein from the hemolymph of *Locusta migratoria*. *J. Biol. Chem.* **271** (49), 31756–31762, <https://doi.org/10.1074/jbc.271.49.31756>
- Brettell, L.E., Martin, S.J. (2017) Oldest *Varroa* tolerant honey bee population provides insight into the origins of the global decline of honey bees. *Sci. Rep.* **7** (45953), <https://doi.org/10.1038/srep45953>
- Brosnan, J.T., Brosnan M.E. (2006) Branched-chain amino acids: enzyme and substrate regulation. *J. Nutr.* **136** (1), 207S–211S
- Burmester, T., Scheller, K. (1999) Ligands and receptors: common theme in insect storage protein transport. *Naturwissenschaften* **86** (10), 468–474
- Cardoen, D., Ernst, U.R., Boerjan, B., Bogaerts, A., Formesyn, E., et al. (2012) Worker honeybee sterility: a proteomic analysis of suppressed ovary activation. *J. Proteome Res.* **11** (5), 2838–2850, <https://doi.org/10.1021/pr201222s>
- Chan, Q.W., Howes, C.G., Foster, L.J. (2006) Quantitative comparison of caste differences in honeybee hemolymph. *Mol. Cell. Proteomics* **5** (12), 2252–2262, <https://doi.org/10.1074/mcp.M600197-MCP200>
- Chen, Y.P., Higgins, J.A., Feldlaufer, M.F. (2005) Quantitative real-time reverse transcription-PCR analysis of deformed wing virus infection in the honeybee (*Apis mellifera* L.). *Appl. Environ. Microbiol.* **71** (1), 436–441, <https://doi.org/10.1128/AEM.71.1.436-441.2005>
- Chen, Y.P., Pettis, J.S., Collins, A., Feldlaufer, M.F. (2006) Prevalence and transmission of honeybee viruses. *Appl. Environ. Microbiol.* **72** (1), 606–611, <https://doi.org/10.1128/AEM.72.1.606-611.2006>

- Cunha, A.D., Nascimento, A.M., Guidugli, K.R., Simões, Z.L., Bitondi, M.M. (2005) Molecular cloning and expression of a hexamerin cDNA from the honey bee, *Apis mellifera*. *J. Insect. Physiol.* **51** (10), 1135–1147, <https://doi.org/10.1016/j.jinsphys.2005.06.004>
- Dainat, B., Evans, J.D., Chen, Y.P., Gauthier, L., Neumann, P. (2012) Dead or alive: deformed wing virus and *Varroa destructor* reduce the life span of winter honeybees. *Appl. Environ. Microbiol.* **78** (4), 981–987, <https://doi.org/10.1128/AEM.06537-11>
- Dautel, F., Kalkhof, S., Trump, S., Lehmann, I., Beyer, A., et al. (2011) Large-scale 2-D DIGE studies - Guidelines to overcome pitfalls and challenges along the experimental procedure. *JIOMICS* **1** (1), 170–179, <https://doi.org/10.5584/jiomics.v1i1.50>
- De Jong, D., De Jong, P.H., Goncalves, L. S. (1982) Weight loss and other damage to developing worker honeybees from infestation with *Varroa jacobsoni*. *J. Apic. Res.* **21** (3), 165–167
- De Miranda, J.R., Genersch, E. (2010) Deformed wing virus. *J. Invertebr. Pathol.* **103** (1), S48–61, <https://doi.org/10.1016/j.jip.2009.06.012>
- Di Prisco, G., Annoscia, D., Margiotta, M., Ferrara, R., Varricchio, P., et al. (2016) A mutualistic symbiosis between a parasitic mite and a pathogenic virus undermines honey bee immunity and health. *Proc. Natl. Acad. Sci. U S A.* **113** (12), 3203–3208, <https://doi.org/10.1073/pnas.1523515113>
- Du Rand, E.E., Smit, S., Beukes, M., Apostolides, Z., Pirk, C.W., et al. (2015) Detoxification mechanisms of honey bees (*Apis mellifera*) resulting in tolerance of dietary nicotine. *Sci. Rep.* <https://doi.org/10.1038/srep11779>
- Duay, P., De Jong, D., Engels, W. (2003) Weight loss in drone pupae (*Apis mellifera*) multiply infested by *Varroa destructor* mites. *Apidologie* **34** (1), 61–65
- Erban, T., Jedelsky, P.L., Titera, D. (2013) Two-dimensional proteomic analysis of honeybee, *Apis mellifera*, winter worker hemolymph. *Apidologie* **44** (4), 404–418, <https://doi.org/10.1007/s13592-012-0190-5>
- Erban, T., Petrova, D., Harant, K., Jedelsky, P.L., Titera, D. (2014) Two-dimensional gel proteomic analysis of honeybee, *Apis mellifera*, worker red-eye pupa hemolymph. *Apidologie* **45** (1), 53–57, <https://doi.org/10.1007/s13592-013-0230-9>
- Erban, T., Harant, K., Hubalek, M., Vitamvas, P., Kamler, M., et al. (2015) In-depth proteomic analysis of *Varroa destructor*: Detection of DWV-complex, ABPV, VdMLV and honeybee proteins in the mite. *Sci. Rep.* **11** (5), 13907, <https://doi.org/10.1038/srep13907>
- Erban, T., Harant, K., Kamler, M., Markovic, M., Titera, D. (2016) Detailed proteome mapping of newly emerged honeybee worker hemolymph and comparison with the red-eye pupal stage. *Apidologie* **47** (6), 805–817, <https://doi.org/10.1007/s13592-016-0437-7>
- Feng, M., Ramadan, H., Han, B., Fang, Y., Li, J. (2014) Hemolymph proteome changes during worker brood development match the biological divergences between western honey bees (*Apis mellifera*) and eastern honey bees (*Apis cerana*). *BMC Genomics* **5** (15), 563, <https://doi.org/10.1186/1471-2164-15-563>
- Fuchikawa, T., Beer, K., Linke-Winnebeck, C., Ben-David, R., Kotowoy, A., et al. (2017). Neuronal circadian clock protein oscillations are similar in behaviourally rhythmic forager honeybees and in arrhythmic nurses. *Open Biol.* **7** (6), 170047, <https://doi.org/10.1098/rsob.170047>
- Gasteiger, E., Hoogland, C., Gattiker, A., Duvaud, S., Wilkins, M.R., et al. (2005) Protein identification and analysis tools on the ExPASy Server, in: Walker, J. M. (Ed), *The proteomics protocols handbook*. Humana Press, New York City, pp. 571–607
- Gätschenberger, H., Azzami, K., Tautz, J., Beier, H. (2013) Antibacterial immune competence of honey bees (*Apis mellifera*) is adapted to different life stages and environmental risks. *PLoS One.* **8** (6), e66415, <https://doi.org/10.1371/journal.pone.0066415>
- Gilliam, M., Jackson, K.K. (1972) Enzymes in honey bee (*Apis mellifera* L.) hemolymph. *Comp. Biochem. Physiol. B.* **42** (3), 423–427, [https://doi.org/10.1016/0305-0491\(72\)90258-1](https://doi.org/10.1016/0305-0491(72)90258-1)
- Guidugli, K.R., Hepperle, C., Hartfelder, K. (2004) A member of the short-chain dehydrogenase/reductase (SDR) superfamily is a target of the ecdysone response in honey bee (*Apis mellifera*) caste development. *Apidologie* **35**, 37–47, <https://doi.org/10.1051/apido:2003068>
- Hu, H., Bienefeld, K., Wegener, J., Zautke, F., Hao, Y., et al. (2016) Proteome analysis of the hemolymph, mushroom body, and antenna provides novel insight into honeybee resistance against *Varroa* infestation. *J. Proteome Res.* **15** (8), 2841–2854, <https://doi.org/10.1021/acs.jproteome.6b00423>
- Iovinella, I., McAfee, A., Mastrobuoni, G., Kempa, S., Foster, L.J., et al. (2018) Proteomic analysis of chemosensory organs in the honey bee parasite *Varroa destructor*: A comprehensive examination of the potential carriers for semiochemicals. *J. Proteomics* **15** (181), 131–141, <https://doi.org/10.1016/j.jprot.2018.04.009>
- Jamroz, R. C., Beintema, J. J., Stam, W. T., Bradfield, J. Y. (1996) Aromatic hexamerin subunit from adult female cockroaches (*Blaberus discoidalis*): molecular cloning, suppression by juvenile hormone, and evolutionary perspectives. *J. Insect. Physiol.* **42** (2), 115–124
- Ji, T., Shen, F., Liu, Z., Yin, L., Shen, J., et al. (2015) Comparative proteomic analysis reveals mite (*Varroa destructor*) resistance-related proteins in Eastern honeybees (*Apis cerana*). *Genet. Mol. Res.* **14** (3), 10103–10118, <https://doi.org/10.4238/2015.August.21.18>
- Kalynych, S., Pridal, A., Pálková, L., Levčanský, Y., de Miranda, J.R., et al. (2016) Virion structure of Iflavirus Slow Bee paralysis virus at 2.6-angstrom resolution. *J. Virol.* **90** (16), 7444–7455, <https://doi.org/10.1128/JVI.00680-16>
- Koleoglu, G., Goodwin, P.H., Reyes-Quintana, M., Hamiduzzaman, M.M., Guzman-Novoa, E. (2018) *Varroa destructor* parasitism reduces hemocyte concentrations and prophenol oxidase gene expression in bees from two populations. *Parasitol. Res.* **117** (4), 1175–1183, <https://doi.org/10.1007/s00436-018-5796-8>
- Kralj, J., Fuchs, S. (2006) Parasitic *Varroa destructor* mites influence flight duration and homing ability of infested

- Apis mellifera* foragers. *Apidologie* **37** (5), 577–587, <https://doi.org/10.1051/apido:2006040>
- Kunieda, T., Fujiyuki, T., Kucharski, R., Foret, S., Ament, S.A., et al. (2006). Carbohydrate metabolism genes and pathways in insects: insights from the honey bee genome. *Insect Mol. Biol.* **15** (5), 563–576, <https://doi.org/10.1111/j.1365-2583.2006.00677.x>
- Leal, W.S. (2013) Odorant reception in insects: roles of receptors, binding proteins, and degrading enzymes. *Annu. Rev. Entomol.* **58**, 373–91, <https://doi.org/10.1146/annurev-ento-120811-153635>
- Levenbook, L. (1985) Insect storage proteins, in: Kerkut, G. A. and Gilbert, L. I., (Eds.), *Comprehensive insect physiology biochemistry and pharmacology*. Pergamon Press, Oxford, pp. 277–316.
- Li, Z., An, X.K., Liu, Y.D., Hou, M.L. (2016) Transcriptomic and expression analysis of the salivary glands in white-backed planthoppers, *Sogatella furcifera*. *PloS One*, **11** (7), e0159393, <https://doi.org/10.1371/journal.pone.0159393>
- Marchler-Bauer, A., Zheng, C.J., Chitsaz, F., Derbyshire, M.K., Geer, L.Y., et al. (2013) CDD: conserved domains and protein three-dimensional structure. *Nucleic Acids Res.* **41**, D348–D352, <https://doi.org/10.1093/nar/gks1243>
- Martins, J.R., Bitondi, M.M. (2012) Nuclear immunolocalization of hexamerins in the fat body of metamorphosing honey bees. *Insects* **3** (4), 1039–1055, <https://doi.org/10.3390/insects3041039>
- Martins, J. R., Nunes, F. M., Cristino, A. S., Simões, Z. L., Bitondi, M. M. (2010). The four hexamerin genes in the honey bee: structure, molecular evolution and function deduced from expression patterns in queens, workers and drones. *BMC Mol. Biol.* **11** (23), <https://doi.org/10.1186/1471-2199-11-23>
- Martins, J. R., Anhezini, L., Dallacqua, R. P., Simões, Z. L., Bitondi, M. M. (2011). A honey bee hexamerin, HEX 70a, is likely to play an intranuclear role in developing and mature ovarioles and testioles. *PloS One* **6** (12), e29006, <https://doi.org/10.1371/journal.pone.0029006>
- McAfee, A., Chan, Q.W.T., Evans, J., Foster, L.J. (2017) A *Varroa destructor* protein atlas reveals molecular underpinnings of developmental transitions and sexual differentiation. *Mol. Cell Proteomics* **16** (12), 2125–2137, <https://doi.org/10.1074/mcp.RA117.000104>
- Molloy, M., McDowell M.T. (2005) Two-dimensional gel electrophoresis. *Sep. Sci. Technol.* **7**, 123–145, [https://doi.org/10.1016/S0149-6395\(05\)80009-1](https://doi.org/10.1016/S0149-6395(05)80009-1)
- Mordecai, G.J., Brettell, L.E., Pachori, P., Villalobos, E.M., Martin, S.J., et al. (2016) Moku virus; a new Iflavirus found in wasps, honey bees and *Varroa*. *Sci. Rep.* **7** (6), 34983, <https://doi.org/10.1038/srep34983>
- Nazzi, F., Le Conte, Y. (2016) Ecology of *Varroa destructor*, the Major Ectoparasite of the Western Honey Bee, *Apis mellifera*. *Annu. Rev. Entomol.* **61**, 417–432, <https://doi.org/10.1146/annurev-ento-010715-023731>
- Oldroyd, B.P. (1999) Coevolution while you wait: *Varroa jacobsoni*, a new parasite of western honey bees. *Trends Ecol. Evol.* **14** (8), 312–315, [https://doi.org/10.1016/S0169-5347\(99\)01613-4](https://doi.org/10.1016/S0169-5347(99)01613-4)
- Parker, R., Guarna, M.M., Melathopoulos, A.P., Moon, K.M., White, R., et al. (2012) Correlation of proteome-wide changes with social immunity behaviors provides insight into resistance to the parasitic mite, *Varroa destructor*, in the honey bee (*Apis mellifera*). *Genome Biol.* **13** (9), R81, <https://doi.org/10.1186/gb-2012-13-9-r81>
- Pelosi, P., Zhou, J.J., Ban, L.P., Calvello, M. (2006) Soluble proteins in insect chemical communication. *Cell. Mol. Life Sci.* **63** (14), 1658–1676, <https://doi.org/10.1007/s00018-005-5607-0>
- Ramsey, S. D., Ochoa, R., Bauchan, G., Gulbranson, C., Mowery, J.D., et al. (2019) *Varroa destructor* feeds primarily on honey bee fat body tissue and not hemolymph. *Proc. Natl. Acad. Sci. U. S. A.* **116** (5), 1792–1801, <https://doi.org/10.1073/pnas.1818371116>
- Randolt, K., Gimple, O., Geissendörfer, J., Reinders, J., Prusko, C., et al. (2008) Immune-related proteins induced in the hemolymph after aseptic and septic injury differ in honey bee worker larvae and adults. *Arch. Insect Biochem. Physiol.* **69** (4), 155–167, <https://doi.org/10.1002/arch.20269>
- Ryabov, E.V., Wood, G.R., Fannon, J.M., Moore, J.D., Bull, J.C., et al. (2014) A virulent strain of deformed wing virus (DWV) of honeybees (*Apis mellifera*) prevails after *Varroa destructor*-mediated, or in vitro, transmission. *PLoS Pathog.* **10** (6), <https://doi.org/10.1371/journal.ppat.1004230>
- Ryabov, E.V., Fannon, J.M., Moore J.D., Wood, G.R., Evans, D.J. (2016) The Iflaviruses Sacbrood virus and Deformed wing virus evoke different transcriptional responses in the honeybee which may facilitate their horizontal or vertical transmission. *PeerJ* **18** (4), e1591, <https://doi.org/10.7717/peerj.1591>
- Słowińska, M., Liszewska, E., Nynca, J., Bukowska, J., Hejmej, A., et al. (2014) Isolation and characterization of an ovinhibitor, a multidomain Kazal-like inhibitor from turkey (*Meleagris gallopavo*) seminal plasma. *Biol. Reprod.* **91** (5), 108, <https://doi.org/10.1095/biolreprod.114.118836>
- Słowińska, M., Kozłowski K., Jankowski J., Ciereszko A. (2015) Proteomic analysis of white and yellow seminal plasma in turkeys (*Meleagris gallopavo*). *J. Anim. Sci.* **93** (6), 2785–2795, <https://doi.org/10.2527/jas.2015-8912>
- Surlis, C., Carolan, J.C., Coffey, M., Kavanagh, K. (2017) Quantitative proteomics reveals divergent responses in *Apis mellifera* worker and drone pupae to parasitization by *Varroa destructor*. *J. Insect Physiol.* **107**, 291–301
- Telfer, W.H., Kunkel, J.G. (1991) The function and evolution of insect storage hexamers. *Annu. Rev. Entomol.* **36**, 205–228, <https://doi.org/10.1146/annurev-ent.36.010191.001225>
- Tonge, R., Shaw, J., Middleton, B., Rowlinson, R., Rayner, S., et al. (2001) Validation and development of fluorescence two-dimensional differential gel



- electrophoresis proteomics technology. *Proteomics* **1** (3), 377–396, [https://doi.org/10.1002/1615-9861\(200103\)1:3<377::AID-PROT377>3.0.CO;2-6](https://doi.org/10.1002/1615-9861(200103)1:3<377::AID-PROT377>3.0.CO;2-6)
- Tripathi, R. K., Dixon, S.E. (1969). Changes in some hemolymph dehydrogenase isozymes of the female honeybee, *Apis mellifera* L., during caste development. *Can. J. Zool.* **47**, 763–770
- Vierstraete, E., Verleyen, P., Baggerman, G., D'Hertog, W., Van den Bergh, G., et al. (2004) A proteomic approach for the analysis of instantly released wound and immune proteins in *Drosophila melanogaster* hemolymph. *Proc. Natl. Acad. Sci. U. S. A.* **13** (101), 470–475, <https://doi.org/10.1073/pnas.0304567101>
- Villalobos, E.M. (2016) Ecology. The mite that jumped, the bee that traveled, the disease that followed. *Science* **351** (6273), 554–556, <https://doi.org/10.1126/science.aaf0938>
- Vizcaino, J.A., Csordas, A., del-Toro, N., Dianas, J.A., Griss, J., et al. (2016) 2016 update of the PRIDE database and its related tools. *Nucleic Acids Res.* **44** (22), 11033, <https://doi.org/10.1093/nar/gkw880>
- Vogt, R.G. (2003) Biochemical diversity of odor detection: OBPs, ODEs and SNMPs. in: Blomquist, G.J. and Vogt, R.G. (Eds.), *Insect pheromone biochemistry and molecular biology*. Elsevier Academic Press, London, pp. 391–446
- Wilfert, L., Long, G., Leggett, H.C., Schmid-Hempel, P., Butlin, R., et al. (2016) Deformed wing virus is a recent global epidemic in honeybees driven by *Varroa* mites. *Science* **351** (6273), 594–597, <https://doi.org/10.1126/science.aac9976>
- Yue, C., Genersch, E. (2005) RT-PCR analysis of Deformed wing virus in honeybees (*Apis mellifera*) and mites (*Varroa destructor*). *J. Gen. Virol.* **86** (Pt 12), 3419–3424, <https://doi.org/10.1099/vir.0.81401-0>
- Zakharkin, S. O., Headley, V. V., Kumar, N. K., Buck, N. A., Wheeler, D.E., et al. (2001) Female specific expression of a hexamerin gene in larvae of an autogenous mosquito. *Eur. J. Biochem.* **268** (22), 5713–5722
- Zhao, X., Gou, X., Qin, Z., Li, D., Wang, Y., et al. (2017) Identification and expression of cuticular protein genes based on *Locusta migratoria* transcriptome. *Sci. Rep.* **7**, <https://doi.org/10.1038/srep45462>
- Zhu, J., Iovinella, I., Dani, F.R., Liu, Y.L., Huang, L.Q., et al. (2016) Conserved chemosensory proteins in the proboscis and eyes of *Lepidoptera*. *Int. J. Biol. Sci.* **12** (11), 1394–1404, <https://doi.org/10.7150/ijbs.16517>
- Zufelato, M.S., Lourenço, A.P., Simões, Z.L., Jorge, J.A., Bitondi, M.M. (2004) Phenoloxidase activity in *Apis mellifera* honey bee pupae, and ecdysteroid-dependent expression of the prophenoloxidase mRNA. *Insect Biochem. Mol. Biol.* **34** (12), 1257–1268, <https://doi.org/10.1016/j.ibmb.2004.08.005>

**Publisher's note** Springer Nature remains neutral with regard to jurisdictional claims in published maps and institutional affiliations.